Immobile IP_3 Receptor Clusters: Building Blocks For IP_3-Evoked Ca^{2+} Signals

Colin W. Taylor[1], Nagendra Babu Thillaiappan and David L. Prole

Department of Pharmacology, Tennis Court Road, Cambridge, CB2 1PD, United Kingdom.

[1]Author for correspondence: cwt1000@cam.ac.uk

Co-regulation of IP_3 receptors (IP_3Rs) by IP_3 and cytosolic Ca^{2+} allows them to mediate regenerative signals, amongst which are Ca^{2+} puffs. These reflect the near-simultaneous opening of a few IP_3Rs within a small cluster. A long-standing conundrum is the observation that while most IP_3Rs appear to be mobile, Ca^{2+} puffs repeatedly initiate from a limited number of fixed sites. Using gene-editing to attach GFP to endogenous IP_3Rs in HeLa cells has allowed the distribution of IP_3Rs and the Ca^{2+} signals they evoke to be imaged simultaneously. This approach shows that most endogenous IP_3Rs are loosely assembled into small clusters, most of which are mobile. However, the Ca^{2+} puffs evoked by histamine or photolysis of caged IP_3 invariably initiated at immobile IP_3R clusters adjacent to the plasma membrane (PM). Hence, only a small fraction of cellular IP_3Rs are 'licensed' to respond. The licensed IP_3R clusters sit alongside the sites where store-operated Ca^{2+} entry (SOCE) occurs, suggesting that the IP_3Rs may allow local regulation of SOCE.

Keywords: Ca^{2+} signal, Ca^{2+}-induced Ca^{2+} release, endoplasmic reticulum, IP_3 receptor, spatial organization, store-operated Ca^{2+} entry.

CONTENTS

INTRODUCTION

Inositol 1,4,5-trisphosphate receptors (IP_3Rs) and their cousins, the ryanodine receptors (RyRs), are the largest of all ion channels. Each forms a large-conductance Ca^{2+} channel with relatively weak selectivity for Ca^{2+} over K^+ (Van Petegem 2014, Foskett et al. 2007). Both of these major families of intracellular Ca^{2+} channels are expressed predominantly within the endoplasmic or sarcoplasmic reticulum (ER or SR), where the functional channel is assembled from four closely related subunits. For IP_3Rs, the channel can comprise four identical subunits or a mixture drawn from the products of the three IP_3R genes and their splice variants (Joseph et al. 2000). RyRs are invariably homomeric. The IP_3R subtypes differ in their expression between cell types, in their subcellular distributions, their association with accessory proteins and in their affinities for IP_3 and modulation by additional intracellular signals (Prole & Taylor 2016). The subtypes may also fulfil different biological roles. However, the similarities between IP_3R subtypes are more striking than the differences. The most important of the shared features is the co-regulation of all IP_3Rs by IP_3 and cytosolic Ca^{2+}: both ligands are required for the IP_3R channel to open. The simplest scheme envisages that binding of IP_3 primes IP_3Rs to bind Ca^{2+}, with Ca^{2+} binding then triggering channel gating (**Fig. 1A**). This interplay is important because it endows IP_3Rs with a capacity to amplify, through Ca^{2+}-induced Ca^{2+} release (CICR), the Ca^{2+} signals evoked by IP_3Rs or other Ca^{2+} channels. Higher concentrations of cytosolic Ca^{2+} inhibit IP_3Rs. There is, therefore, a biphasic dependence of IP_3R gating on cytosolic Ca^{2+} concentration: low Ca^{2+} concentrations are stimulatory, while higher concentrations inhibit. RyRs are also biphasically regulated by cytosolic Ca^{2+} (Van Petegem 2016). It is worth noting, since the observations are still cited, that it had been suggested that IP_3R2 and IP_3R3 were not biphasically regulated by cytosolic Ca^{2+} (Hagar et al. 1998, Ramos-Franco et al. 1998). However, subsequent work established that all IP_3Rs are biphasically regulated by cytosolic Ca^{2+} (Foskett et al. 2007, Taylor & Tovey 2012), although there are subtle differences between IP_3R subtypes in the interplay between IP_3 and Ca^{2+}.

The structural basis of IP_3R activation has been most explored for IP_3R1, but the considerable amino acid sequence similarity between IP_3R subtypes suggests that the mechanisms of activation are likely to be similar for all subtypes. Indeed, the basic architecture of the activation mechanisms is probably similar for IP_3Rs and RyRs (Seo et al. 2012, Van Petegem 2016). For IP_3Rs, activation begins when IP_3 binds to the clam-like IP_3-binding core (IBC), which lies towards the N-terminal of the primary sequence of each subunit (**Fig. 1B**). The IBCs of all four subunits must bind IP_3 before the channel can open

(Alzayady et al. 2016). The 4- and 5-phosphate groups of IP_3, which are essential features of all IP_3R ligands, interact with basic residues lining opposite sides of the inner surface of the clam (Bosanac et al. 2002). This allows IP_3 binding to partially close the clam. Since one side of the clam, the α-domain, adheres tightly to the N-terminal domain of the IP_3R (the so-called suppressor domain, SD), clam closure causes movement of the SD. We suggest that this movement weakens interactions between IP_3R subunits, leading ultimately to channel gating (Seo et al. 2012). However, details of the structural links between the initial conformational changes around the IBC and SD, Ca^{2+} binding, and dilation of the pore that allows Ca^{2+} to pass from the ER into the cytosol, are not yet resolved. A major step towards revealing these details is the cryo-EM structure of IP_3R1 in a closed state (Fan et al. 2015). A notable feature of this structure, which may point the way towards a gating mechanism, is the rod-like α-helical C-terminal domain, which extends directly from TMD6, through a perpendicular linking domain, to make contact with the SD of an adjacent subunit (Fan et al. 2015).

The most pertinent points for subsequent discussion are the obligate co-regulation of IP_3Rs by IP_3 and cytosolic Ca^{2+}; the large Ca^{2+} conductance of IP_3Rs (Foskett et al. 2007); the large size of an IP_3R (11,000 residues, ~1.2 MDa) with its mushroom-like cytosolic region extending some 20 nm from the ER membrane (Fan et al. 2015); and the observation that neither RyRs nor IP_3Rs are randomly distributed within intracellular membranes (Franzini-Armstrong 2018, Thillaiappan et al. 2017, Jayasinghe et al. 2018).

RECRUITMENT OF CA^{2+} SIGNALS BY IP_3-REGULATED CICR

High-resolution optical imaging, first with confocal microscopy and then with total internal reflection fluorescence microscopy (TIRFM), has revealed the subcellular organization of IP_3-evoked Ca^{2+} signals in cells loaded with a fluorescent Ca^{2+} indicator and EGTA to restrain the regenerative propagation of Ca^{2+} signals by CICR (Bootman et al. 1997, Wiltgen et al. 2010, Parker & Smith 2010). These 'optical patch-clamp' methods resolve the brief openings of individual IP_3Rs (as 'Ca^{2+} blips'); the co-ordinated opening of several (typically fewer than 10) IP_3Rs within small clusters ('Ca^{2+} puffs'); and the regenerative propagation of intracellular Ca^{2+} waves, which initiate more frequently as the IP_3 concentration increases (Smith & Parker 2009, Thurley et al. 2014). This hierarchy of Ca^{2+} release events is assumed to arise from CICR as higher concentrations of IP_3 progressively prime more IP_3Rs to respond to Ca^{2+} diffusing to them from nearby active IP_3Rs (**Fig. 1C**). The functional significance of the hierarchy comes from the changing nature of the Ca^{2+} signals as the stimulus intensity increases, and the opportunities that provides for encoding Ca^{2+} signals in

both spatial and temporal domains. Hence, the Ca^{2+} signal evolves from large focal increases in cytosolic [Ca^{2+}] delivered to targets adjacent to IP_3Rs, to a global signal that can activate more remote targets, and these global signals can encode stimulus intensity in the frequency of the resulting Ca^{2+} spikes (Thurley et al. 2014). The extent to which IP_3-evoked Ca^{2+} signals are amplified by this CICR mechanism, and so progress through the hierarchical pathway, depends on both the concentration of IP_3 and the separation of IP_3Rs.

Where Ca^{2+} blips have been resolved, they arise from sites that appear either immobile or to move with diffusion coefficients ($D = 0.003\ \mu m^2 s^{-1}$) (Wiltgen et al. 2010) at least ten-times slower than those of IP_3Rs determined from fluorescence recovery after photobleaching (FRAP) or single-particle tracking of tagged IP_3Rs (Smith et al. 2014, Thillaiappan et al. 2017). It is not yet clear whether Ca^{2+} blips arise from lone IP_3Rs or from IP_3Rs within clusters that fail to ignite the activity of their neighbours. Ca^{2+} puffs also initiate at sites that remain immobile for many minutes (Wiltgen et al. 2010, Bootman et al. 1997, Keebler & Taylor 2017, Thillaiappan et al. 2017). The pioneering studies of IP_3R puffs suggested there were no more than a handful of initiation sites per cell (Bootman et al. 1997, Smith et al. 2014, see Smith & Parker 2009), but recent work suggests they may be more abundant with perhaps a hundred sites per cell (Keebler & Taylor 2017). Nevertheless, it is clear that Ca^{2+} puffs repeatedly initiate at sites that remain immobile for many minutes, and which include only a small fraction of the total complement of IP_3Rs. There is, therefore, a conundrum in that most IP_3Rs (typically ~70%) appear to be mobile, yet IP_3-evoked Ca^{2+} signals initiate at fixed sites, leading Parker and his colleagues to speculate that anchoring of immobile IP_3Rs into clusters may prime them to respond to IP_3 (Parker & Smith 2010, Smith et al. 2014). To gain further insight into this problem, we used gene-editing to attach enhanced green fluorescent protein (GFP) to the endogenous IP_3R1 of HeLa cells (Thillaiappan et al. 2017). We demonstrated that all IP_3R1s, the major subtype in HeLa cells, were tagged with GFP, the tagged IP_3R1s were functional and assembled with other IP_3R subtypes, and they were expressed in clusters within ER membranes. Subsequent sections of this short review focus on our analyses of these tagged endogenous IP_3Rs insofar as they illuminate our understanding of the relationship between the geography of IP_3Rs and the Ca^{2+} signals they elicit.

WHAT IS AN IP_3 RECEPTOR CLUSTER?

Functional analyses of Ca^{2+} puffs (Dickinson et al. 2012), single-particle tracking of over-expressed mEos2-IP_3R1 (Smith et al. 2014) and patch-clamp recordings from the outer

nuclear envelope (Rahman et al. 2009, Vais et al. 2011, Rahman et al. 2011) suggest that typical puff sites are likely to include 2-9 functional IP_3Rs. There is, however, considerable heterogeneity in the number of active IP_3Rs, both between sites and between successive Ca^{2+} puffs at the same site (Smith & Parker 2009). This suggests that not all IP_3Rs within a cluster are recruited during each Ca^{2+} puff.

Our single-step photobleaching analyses of endogenous GFP-IP_3R1 in HeLa cells suggest that most IP_3Rs form clusters, with up to ~40 IP_3Rs in each, and a mean of ~8 IP_3Rs per cluster (Thillaiappan et al., 2017) (**Fig. 2A**). The dimensions of a cluster, typically several 100 nm across, are similar to the dimensions estimated from a single-particle tracking analysis (~400 nm) (Smith et al. 2014). These small IP_3R clusters, which we suggest may be the elementary structural units of IP_3R signalling, are expressed throughout the cell. A surprising observation is the apparent independence of each cluster. There is no evident mixing of IP_3Rs between mobile and immobile clusters, and we observe clusters apparently moving past each other without losing their identities. Hence, once IP_3Rs are assembled into a cluster, it seems to be a long-lasting relationship. Super-resolution analyses of the distribution of IP_3Rs within clusters suggests that many of the component IP_3Rs are too far apart to interact with each other directly (**Fig. 2A**). We suggest, therefore, that IP_3R clusters are loose confederations held together by scaffolding complexes that might involve cytosolic or ER proteins, lipid microdomains, or contacts between ER and other organelles (**Fig. 2A**). The notion that IP_3Rs might be relatively loosely distributed within their stable clusters sits comfortably with several features of Ca^{2+} puffs. Firstly, although the rising phase of Ca^{2+} puffs is usually very brisk, consistent with rapid recruitment of closely spaced IP_3Rs, it is sometimes possible to discern steps in the rising phase, suggestive of a looser coupling (Smith & Parker 2009). Secondly, and notwithstanding the blurring of signals as Ca^{2+} diffuses away from IP_3Rs, the dimensions of Ca^{2+} puffs (~500 nm) are much larger than needed to accommodate ten or fewer IP_3Rs (each ~20 nm across). Thirdly, although puff sites are immobile, the peak of the Ca^{2+} signal wanders by up to 300 nm within the site during a puff (Wiltgen et al. 2010), suggesting that active IP_3Rs may be as much as 300 nm apart. Finally, even the most mobile of Ca^{2+} blips ($D = 0.003\ \mu m^2 s^{-1}$) (Wiltgen et al. 2010), which may represent IP_3Rs within clusters that fail to ignite a Ca^{2+} puff, would be expected to move only about 35 nm during the typical duration of a Ca^{2+} puff (i.e. well within the confines of the loose cluster). Hence, we suggest that most IP_3Rs, whether mobile or immobile, are corralled into loose confederations by scaffolding complexes that typically hold ~8 IP_3Rs in a long-lasting relationship.

We concluded from our previous patch-clamp analyses of IP_3Rs in the outer nuclear envelope, which is continuous with the ER, that low concentrations of IP_3 cause IP_3Rs to assemble into small clusters (Rahman et al. 2009, Rahman et al. 2011). Others have challenged this conclusion by suggesting that IP_3R clusters assemble without the need to increase the intracellular IP_3 concentration (Vais et al. 2011, Smith et al. 2009b), and our results from HeLa cells also show that stable IP_3R clusters are present in unstimulated cells (Thillaiappan et al. 2017). How might these observations be reconciled? It may be that the nuclear envelope is not an appropriate model for the ER, or basal levels of IP_3 may be sufficient to ensure assembly of IP_3R clusters in unstimulated cells (Smith et al. 2009b). However, a more attractive possibility, which we have yet to address experimentally, is that most IP_3Rs are already assembled into loose corrals in unstimulated cells, and IP_3 then promotes tighter clustering within the corral. Although preliminary analyses failed to provide support for this scheme (Smith et al. 2014), it deserves closer attention since such local 'huddling' would not increase the size of each pre-formed cluster, but it would be expected to improve the CICR-mediated recruitment of IP_3Rs within a cluster. Hence, IP_3 might initiate Ca^{2+} puffs by stimulating gating of IP_3Rs and by enhancing CICR by causing loosely pre-clustered IP_3Rs to huddle.

CA^{2+} PUFFS OCCUR AT IMMOBILE IP_3 RECEPTOR CLUSTERS NEAR THE PLASMA MEMBRANE

Both direct measurements, using FRAP (Fukatsu et al. 2004, Pantazaka & Taylor 2011, Ferreri-Jacobia et al. 2005) or single-particle tracking (Smith et al. 2014, Thillaiappan et al. 2017), and evidence that stimuli can regulate IP_3R clustering (Wilson et al. 1998, Tateishi et al. 2005, Iwai et al. 2005, Chalmers et al. 2006, Tojyo et al. 2008, Rahman et al. 2009, Geyer et al. 2015) attest to the mobility of IP_3Rs within ER membranes. Typically, these studies suggest that most IP_3Rs are mobile (mobile fractions, M_f, typically ~70%) and that most movement is by diffusion. A caveat remains that most such studies have observed over-expressed IP_3Rs, with the attendant risk that they may not faithfully report behaviours of endogenous IP_3Rs. Using single-particle tracking of endogenous GFP-IP_3Rs in HeLa cells to record the movement of IP_3R clusters, we observed that most clusters (~70%) were mobile, while the remainder remained immobile for periods of many minutes. Within the population of mobile clusters, most clusters moved by diffusion (D ~0.03 $\mu m^2.s^{-1}$), but a small fraction of the mobile clusters (~10%) moved directionally along microtubules, driven by kinesin and dynein motors (Thillaiappan et al. 2017). Our results are similar to those obtained using

single-particle tracking of over-expressed mEos2-IP_3R1, in suggesting that ~70% of IP_3Rs are mobile, but they differ in that only we observed directional movement along microtubules. The difference may be due to the different cell types used or to over-expression of mEos2-IP_3R1 masking the small number of actively moving IP_3R clusters. The key points are that most native IP_3Rs are clustered, and most of these clusters are mobile.

In HeLa cells, almost all Ca^{2+} puffs initiate close to the plasma membrane (PM) (Thillaiappan et al. 2017), consistent with similar observations in SH-SY5Y cells (Smith et al. 2009a). Furthermore, the pattern was similar whether the Ca^{2+} signals were evoked by histamine to stimulate endogenous signalling pathways, or by photolysis of caged-IP_3 to allow uniform release of IP_3 throughout the cytosol. Indeed, both we (Keebler & Taylor 2017) and others (Lock et al. 2017) have shown that endogenous signalling pathways and photo-released IP_3 activate the same Ca^{2+} puff sites. By simultaneously recording the Ca^{2+} puffs evoked by IP_3 and the underlying distribution of endogenous GFP-IP_3Rs in HeLa cells, we showed that Ca^{2+} puffs initiate only at immobile clusters of IP_3Rs (Thillaiappan et al. 2017). The observation is important, because IP_3R clusters are expressed throughout the cell, not just near the PM, and most IP_3R clusters are mobile. Hence, only a small subset of the few thousand IP_3Rs in a cell, namely those within immobile clusters adjacent to the PM, is 'licensed' to respond to IP_3 (**Fig. 2B**). There must, therefore, be an additional level of regulation of IP_3Rs that endows them with the competence to respond to IP_3. The nature of that regulation has yet to be resolved.

In addition to causing an increase in cytosolic [Ca^{2+}], activation of IP_3Rs also causes a decrease in [Ca^{2+}] within the ER, and that leads to activation of store-operated Ca^{2+} entry (SOCE) (Hogan 2015). The core features of SOCE are now clear: they involve direct interactions between the ER Ca^{2+} sensor, stromal interaction molecule 1 (STIM1), and the PM Ca^{2+} channel, Orai1. Loss of Ca^{2+} from the luminal EF-hands of STIM1 causes STIM1 to cluster and expose cytosolic domains that bind to phosphatidylinositol 4,5-bisphosphate (PIP_2) and Orai1. Binding of STIM1 to Orai opens its channel, allowing Ca^{2+} to flow into the cell. Hence, loss of ER Ca^{2+} causes STIM1 to be captured, through its interaction with PIP_2 and Orai, within narrow junctions where the ER and PM are no more than ~20 nm apart (Hogan 2015, Prakriya & Lewis 2015). Our results from HeLa cells show that the sites to which STIM1 translocates after loss of Ca^{2+} from the ER are immediately adjacent to (but not perfectly coincident with) the immobile near-PM IP_3R clusters that we know to be the sites where Ca^{2+} puffs occur (Thillaiappan et al. 2017). Because IP_3Rs project about 20 nm from the ER membrane (Fan et al. 2015), they may be too large to enter the narrow ER-PM

junctions wherein STIM and Orai interact. This physical exclusion may account for the lack of perfect colocalization of STIM1 with immobile IP_3R clusters, but it leaves unexplained our observation that immobile near-PM IP_3R clusters are preferentially juxtaposed to the ER-PM SOCE junctions (Thillaiappan et al. 2017). Future work will need to identify the tether that positions the licensed IP_3R clusters adjacent to SOCE junctions. We can, however, speculate on the possible physiological significance of the juxtaposition.

We suggest that immobile near-PM IP_3R clusters sit alongside SOCE junctions and face the PM (**Fig. 2B**). Since PIP_2 recruits STIM to ER-PM junctions, we suggest that the licensed IP_3R clusters are located immediately alongside the substrate (PIP_2) from which endogenous signalling pathways will generate IP_3. Activation of SOCE requires substantial loss of Ca^{2+} from the ER (Brandman et al. 2007, Prakriya & Lewis 2015), yet while regulating SOCE the ER must also fulfil numerous additional functions, many of which require luminal Ca^{2+} (Berridge 2002). We speculate that the positioning of licensed IP_3R clusters alongside SOCE junctions might allow IP_3R activation to locally deplete the ER and activate SOCE without trespassing into the other Ca^{2+}-requiring functions of the ER. Finally, SOCE is acutely regulated by Ca^{2+} passing through the low-conductance Orai1 channel (Prakriya & Lewis 2015). If IP_3Rs, with their very large Ca^{2+} conductance, were too close to SOCE junctions, they might disrupt this local feedback regulation. Hence, having the licensed IP_3Rs that will respond to IP_3 alongside, rather than within, SOCE junctions may provide the best compromise between local regulation of SOCE by local depletion of ER Ca^{2+} stores, while retaining acute auto-regulation of SOCE by Ca^{2+} passing through Orai channels (**Fig. 2B**).

CONCLUSIONS

IP_3Rs are co-regulated by IP_3 and cytosolic Ca^{2+}. This allows them to mediate regenerative intracellular Ca^{2+} signals as IP_3 primes IP_3Rs to respond to Ca^{2+} (**Fig. 1C**). Ca^{2+} puffs, which report the near-simultaneous opening of a small number of IP_3Rs within a cluster, are the smallest units of these regenerative Ca^{2+} signals. Each cluster is a loose, but stable, confederation of a small number of IP_3Rs that must be held together by an as yet unidentified scaffold. Most IP_3R clusters are mobile, but only immobile clusters immediately adjacent to the PM initiate Ca^{2+} puffs. The additional signal that provides these licensed IP_3Rs with competence to respond to IP_3 is unknown. Nor is it resolved whether the large population of mobile IP_3R clusters contributes to Ca^{2+} signals evoked by more intense stimulation. Since the licensed IP_3R clusters sit alongside the ER-PM junctions where SOCE occurs, we speculate that they may contribute to local regulation of SOCE.

Acknowledgements: This work was supported by the Wellcome Trust (101844) and Biotechnology and Biological Sciences Research Council (BB/P0053301/1).

REFERENCES

Alzayady, K. J., Wang, L., Chandrasekhar, R., Wagner, L. E., 2nd, Van Petegem, F. and Yule, D. I. (2016) Defining the stoichiometry of inositol 1,4,5-trisphosphate binding required to initiate Ca^{2+} release. *Sci. Signal.,* **9,** ra35.

Berridge, M. J. (2002) The endoplasmic reticulum: a multifunctional signaling organelle. *Cell Calcium,* **32,** 235-249.

Bootman, M. D., Berridge, M. J. and Lipp, P. (1997) Cooking with calcium: the recipes for composing global signals from elementary events. *Cell,* **91,** 367-373.

Bosanac, I., Alattia, J.-R., Mal, T. K. et al. (2002) Structure of the inositol 1,4,5-trisphosphate receptor binding core in complex with its ligand. *Nature,* **420,** 696-700.

Brandman, O., Liou, J., Park, W. S. and Meyer, T. (2007) STIM2 is a feedback regulator that stabilizes basal cytosolic and endoplasmic reticulum Ca^{2+} levels. *Cell,* **131,** 1327-1339.

Chalmers, M., Schell, M. J. and Thorn, P. (2006) Agonist-evoked inositol trisphosphate receptor (IP_3R) clustering is not dependent on changes in the structure of the endoplasmic reticulum. *Biochem. J.,* **394,** 57-66.

Dickinson, G. D., Swaminathan, D. and Parker, I. (2012) The probability of triggering calcium puffs is linearly related to the number of inositol trisphosphate receptors in a cluster. *Biophys. J.,* **102,** 1826-1836.

Fan, G., Baker, M. L., Wang, Z., Baker, M. R., Sinyagovskiy, P. A., Chiu, W., Ludtke, S. J. and Serysheva, II (2015) Gating machinery of $InsP_3R$ channels revealed by electron cryomicroscopy. *Nature,* **527,** 336-341.

Ferreri-Jacobia, M., Mak, D.-O., D. and Foskett, J. K. (2005) Translational mobility of the type 3 inositol 1,4,5-trisphosphate receptor Ca^{2+} release channel in endoplasmic reticulum membrane. *J. Biol. Chem.,* **280,** 3824-3831.

Foskett, J. K., White, C., Cheung, K. H. and Mak, D. O. (2007) Inositol trisphosphate receptor Ca^{2+} release channels. *Physiol. Rev.,* **87,** 593-658.

Franzini-Armstrong, C. (2018) The relationship between form and function throughout the history of excitation-contraction coupling. *J. Gen. Physiol.,* In press.

Fukatsu, K., Bannai, H., Zhang, S., Nakamura, H., Inoue, T. and Mikoshiba, K. (2004) Lateral diffusion of inositol 1,4,5-trisphosphate receptor type 1 is regulated by actin filaments and 4.1N in neuronal dendrites. *J. Biol. Chem.,* **279,** 48976-48982.

Geyer, M., Huang, F., Sun, Y., Vogel, S. M., Malik, A. B., Taylor, C. W. and Komarova, Y. A. (2015) Microtubule-associated protein EB3 regulates IP_3 receptor clustering and Ca^{2+} signaling in endothelial cells. *Cell Rep.,* **12,** 79-89.

Hagar, R. E., Burgstahler, A. D., Nathanson, M. H. and Ehrlich, B. E. (1998) Type III $InsP_3$ receptor channel stays open in the presence of increased calcium. *Nature,* **296,** 81-84.

Hogan, P. G. (2015) The STIM1-ORAI1 microdomain. *Cell Calcium,* **58,** 357-367.

Iwai, M., Tateishi, Y., Hattori, M. et al. (2005) Molecular cloning of mouse type 2 and type 3 inositol 1,4,5-trisphosphate receptors and identification of a novel type 2 receptor splice variant. *J. Biol. Chem.,* **280,** 10305-10317.

Jayasinghe, I., Clowsley, A. H., Lin, R., Lutz, T., Harrison, C., Green, E., Baddeley, D., Di Michele, L. and Soeller, C. (2018) True molecular scale visualization of variable clustering properties of ryanodine receptors. *Cell Rep.,* **22,** 557-567.

Joseph, S. K., Bokkala, S., Boehning, D. and Zeigler, S. (2000) Factors determining the composition of inositol trisphosphate receptor hetero-oligomers expressed in COS cells. *J. Biol. Chem.,* **275,** 16084-16090.

Keebler, M. V. and Taylor, C. W. (2017) Endogenous signalling pathways and caged-IP_3 evoke Ca^{2+} puffs at the same abundant immobile intracellular sites. *J. Cell Sci.,* **130,** 3728-3739.

Lock, J. T., Smith, I. F. and Parker, I. (2017) Comparison of Ca^{2+} puffs evoked by extracellular agonists and photoreleased IP_3. *Cell Calcium,* **63,** 43-47.

Pantazaka, E. and Taylor, C. W. (2011) Differential distribution, clustering and lateral diffusion of subtypes of inositol 1,4,5-trisphosphate receptor. *J. Biol. Chem.,* **286,** 23378-23387.

Parker, I. and Smith, I. F. (2010) Recording single-channel activity of inositol trisphosphate receptors in intact cells with a microscope, not a patch clamp. *J. Gen. Physiol.,* **136,** 119-127.

Prakriya, M. and Lewis, R. S. (2015) Store-operated calcium channels. *Physiol. Rev.,* **95,** 1383-1436.

Prole, D. L. and Taylor, C. W. (2016) Inositol 1,4,5-trisphosphate receptors and their protein partners as signalling hubs. *J. Physiol.,* **594,** 2849-2866.

Rahman, T., Skupin, A., Falcke, M. and Taylor, C. W. (2011) InsP3R channel gating altered by clustering? Rahman *et al.* reply. *Nature,* **478,** E2-E3.

Rahman, T. U., Skupin, A., Falcke, M. and Taylor, C. W. (2009) Clustering of IP_3 receptors by IP_3 retunes their regulation by IP_3 and Ca^{2+}. *Nature,* **458,** 655-659.

Ramos-Franco, J., Fill, M. and Mignery, G. A. (1998) Isoform-specific function of single inositol 1,4,5-trisphosphate receptor channels. *Biophys. J.,* **75,** 834-839.

Seo, M.-D., Velamakanni, S., Ishiyama, N. et al. (2012) Structural and functional conservation of key domains in $InsP_3$ and ryanodine receptors. *Nature,* **483,** 108-112.

Smith, I. F. and Parker, I. (2009) Imaging the quantal substructure of single IP_3R channel activity during Ca^{2+} puffs in intact mammalian cells. *Proc. Natl. Acad. Sci. USA,* **106,** 6404-6409.

Smith, I. F., Swaminathan, D., Dickinson, G. D. and Parker, I. (2014) Single-molecule tracking of inositol trisphosphate receptors reveals different motilities and distributions. *Biophys. J.,* **107,** 834-845.

Smith, I. F., Wiltgen, S. M. and Parker, I. (2009a) Localization of puff sites adjacent to the plasma membrane: functional and spatial characterization of Ca^{2+} signaling in SH-SY5Y cells utilizing membrane-permeant caged IP_3. *Cell Calcium,* **45,** 65-76.

Smith, I. F., Wiltgen, S. M., Shuai, J. and Parker, I. (2009b) Ca^{2+} puffs originate from preestablished stable clusters of inositol trisphosphate receptors. *Sci. Signal.,* **2,** ra77.

Tateishi, Y., Hattori, M., Nakayama, T., Iwai, M., Bannai, H., Nakamura, T., Michikawa, T., Inoue, T. and Mikoshiba, K. (2005) Cluster formation of inositol 1,4,5-trisphosphate receptor requires its transition to open state. *J. Biol. Chem.,* **280,** 6816-6822.

Taylor, C. W. and Tovey, S. C. (2012) IP_3 receptors: toward understanding their activation. *Cold Spring Harb. Persp. Biol.,* **2,** a004010.

Thillaiappan, N. B., Chavda, A. P., Tovey, S. C., Prole, D. L. and Taylor, C. W. (2017) Ca^{2+} signals initiate at immobile IP_3 receptors adjacent to ER-plasma membrane junctions. *Nat. Commun.,* **8,** 1505.

Thurley, K., Tovey, S. C., Moenke, G., Prince, V. L., Meena, A., Thomas, A. P., Skupin, A., Taylor, C. W. and Falcke, M. (2014) Reliable encoding of stimulus intensities within random sequences of intracellular Ca^{2+} spikes. *Sci. Signal.,* **7,** ra59.

Tojyo, Y., Morita, T., Nezu, A. and Tanimura, A. (2008) The clustering of inositol 1,4,5-trisphosphate (IP_3) receptors is triggered by IP_3 binding and facilitated by depletion of the Ca^{2+} store. *J. Pharm. Sci.,* **107,** 138-150.

Vais, H., Foskett, J. K. and Mak, D. O. (2011) $InsP_3R$ channel gating altered by clustering? *Nature,* **478,** E1-E2.

Van Petegem, F. (2014) Ryanodine receptors: allosteric ion channel giants. *J. Mol. Biol.,* **427,** 31-53.

Van Petegem, F. (2016) How to open a ryanodine receptor. *Cell Res.,* **26,** 1073-1074.

Wilson, B. S., Pfeiffer, J. R., Smith, A. J., Oliver, J. M., Oberdorf, J. A. and Wojcikiewicz, R. J. H. (1998) Calcium-dependent clustering of inositol 1,4,5-trisphosphate receptors. *Mol. Biol. Cell,* **9,** 1465-1478.

Wiltgen, S. M., Smith, I. F. and Parker, I. (2010) Superresolution localization of single functional IP_3R channels utilizing Ca^{2+} flux as a readout. *Biophys. J.,* **99,** 437-446.

Figure 1. Hierarchical recruitment of IP_3-evoked Ca^{2+} release. (A) Many receptors in the plasma membrane (PM) stimulate phospholipase C (PLC), with concomitant formation of IP_3. Binding of IP_3 to each of the four subunits of a tetrameric IP_3R primes the IP_3R to bind Ca^{2+}, and that Ca^{2+} binding then triggers channel gating. Co-regulation of IP_3Rs by IP_3 and Ca^{2+} endows them with the capacity to mediate IP_3-regulated Ca^{2+}-induced Ca^{2+} release (CICR). (B) IP_3 binds within the clam-like cleft formed by the α- and β-domains of the IP_3-binding core (IBC), causing partial closure of the clam. This clam closure causes re-orientation of the suppressor domain (SD) and thereby initiates channel gating. The pore of the channel is formed by transmembrane domains (TMD) towards the C-terminal of the primary sequence. Structure from Seo *et al*. (2012). (C) By tuning the gain on CICR by IP_3Rs, IP_3 allows hierarchical recruitment of intracellular Ca^{2+} release events.

Figure 2. Immobile IP_3R clusters at the PM are licensed to respond to IP_3. (A) TIRFM image shows a portion of a HeLa cell in which endogenous IP_3R1s are tagged with GFP; the ER is shown in red. STORM image of a single mobile IP_3R cluster shows the localization of GFP-IP_3R1 in red, and the underlying TIRFM image in green. The yellow box beneath the scale bar shows the approximate dimensions of a single IP_3R tetramer. The image shows that IP_3Rs are often relatively loosely associated within clusters, even though individual clusters retain their individuality for prolonged periods. Single-step photobleaching analyses suggest that IP_3R clusters contain variable numbers of tetrameric IP_3Rs, but with a mean of ~8 IP_3Rs/cluster. Results from Thillaiappan *et al.* (2017). (B) We suggest that most IP_3R clusters are mobile and inactive (red), but licensed IP_3R clusters (green) are immobilized alongside the ER-PM junctions where SOCE occurs. This, we suggest, may allow local regulation of SOCE through local depletion of the ER by licensed IP_3Rs, while retaining acute feedback regulation of SOCE activity by Ca^{2+} passing through Orai channels. See text for further details.

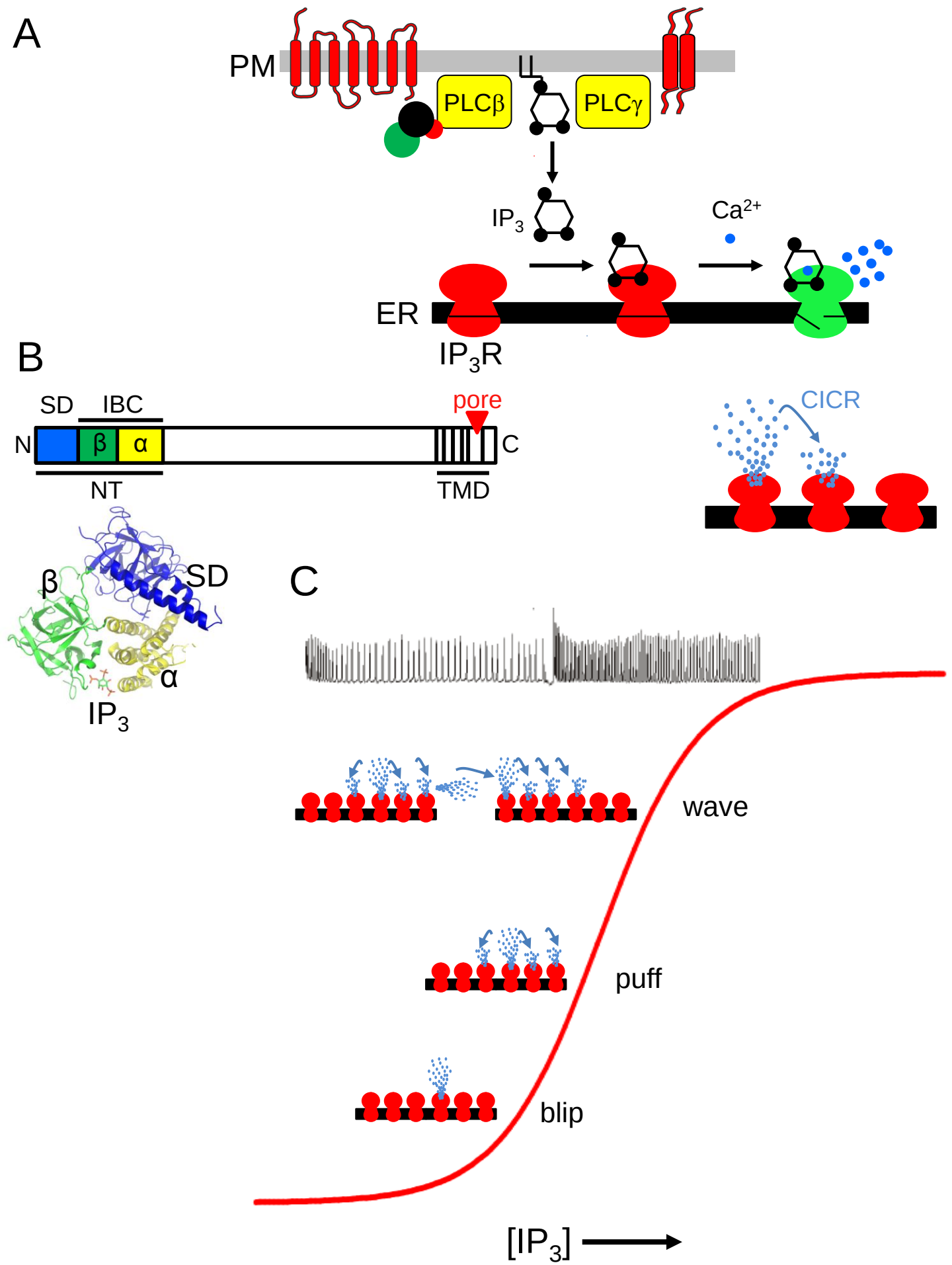

Taylor *et al*, Figure 1

A

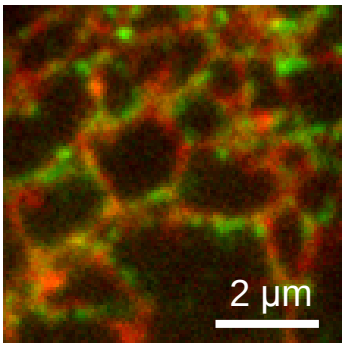

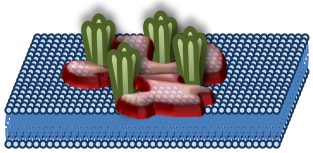

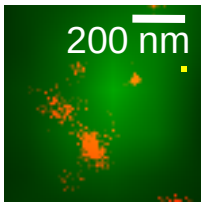

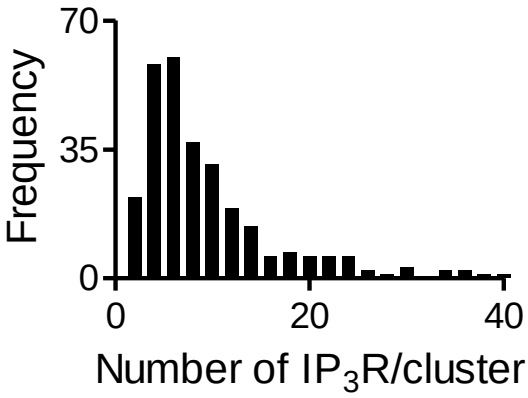

B

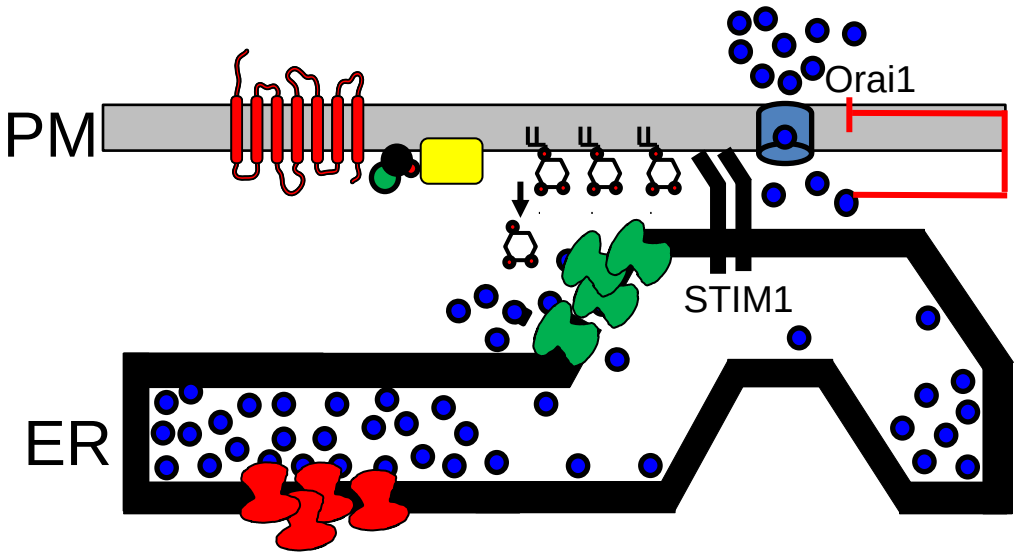

Taylor *et al*, Figure 2